A Method for the Suppression of Multiple Spurious Modes

Jonathan M. Puder, *Student Member, IEEE*, Jeffrey S. Pulskamp, Ryan Q. Rudy, Ronald G. Polcawich, *Senior Member, IEEE*, and Sunil A. Bhave, *Senior Member, IEEE*

***Abstract*— This paper reports on a novel electrode design technique for spur suppression in parallel-plate piezoelectric resonators with minimal impact on the intended vibration mode. To demonstrate this technique, fabricated two-port resonators were designed to optimally excite the first harmonic of length extension in a lead zirconate titanate-on-silicon resonator and suppress chosen higher harmonics. The targeted harmonics have been largely suppressed, while the intended mode experienced no change in magnitude. This is the first step towards a general technique for suppression of an arbitrary mode. [2017-0251]**

***Index Terms*— Spurious mode, piezoelectric, PZT.**

I. Introduction

CONTOUR mode resonators promise high performance with lithographically determined frequencies for monolithic realization of filter banks. Spurious modes are one of the largest obstacles to widespread adoption of contour mode resonator (CMR) technology. Spurious modes distort filter passbands by altering group velocity and ripple, and can violate filter attenuation specification out-of-band. Numerous efforts in the CMR literature to mitigate this problem testify to its pervasiveness and severity across frequencies. Techniques employed include: electrode shaping [1], [2] tether design [3], [4], “mode conversion” [5], and bus design [6]. One of the largest obstacles on the path to commercial success of two related piezoelectric resonator technologies (thin film bulk acoustic resonators (FBARs) and solidly-mounted resonators (SMRs)) was also the spurious mode problem. Techniques employed include frame design, apodization, and the flattening the resonator dispersion curve. An overview of these techniques is given in [7].

Manuscript received October 9, 2017; revised December 9, 2017; accepted January 5, 2018. Date of publication February 15, 2018; date of current version April 2, 2018. This work was supported by the Student Research Participation Program at the U.S. Army Research Laboratory administered by the Oak Ridge Institute for Science and Education through an interagency agreement between the U.S. Department of Energy and U.S. Army Research Laboratory. Subject Editor M. Rais-Zadeh. *(Corresponding author: Jonathan M. Puder.)*

J. M. Puder is with the Sibley School of Mechanical and Aerospace Engineering, Cornell University, Ithaca, NY 14850 USA, and also with General Technical Services, U.S. Army Research Laboratory, Adelphi, MD 20783 USA (e-mail: jmp378@cornell.edu).

J. S. Pulskamp, R. Q. Rudy, and R. G. Polcawich are with the U.S. Army Research Laboratory, Adelphi, MD 20783 USA (e-mail: jeffrey.s.pulskamp.civ@mail.mil; ryan.q.rudy.civ@mail.mil; ronald.g.polcawich.civ@mail.mil).

S. A. Bhave is with the Electrical and Computer Engineering Department, Purdue University, West Lafayette, IN 47907 USA (e-mail: bhave@purdue.edu).

Color versions of one or more of the figures in this paper are available online at http://ieeexplore.ieee.org.

Digital Object Identifier 10.1109/JMEMS.2018.2793100

This paper reports on a unique electrode shaping approach guided by the recently reported Rapid Analytical-FEA Technique (RAFT), which provides analytical insight and speed to the design of resonators while utilizing FEA for accuracy [8]. In this work the designer chooses the modes to be suppressed, and are chosen to be harmonics of length extension for proof-of-concept. Future work towards application to other types of modes and more complex electric fields will be discussed. As such, this work is the first step towards a generalized technique to suppress arbitrary modes.

Section II will cover the theoretical basis and give the condition to completely suppress a mode utilizing a recently reported generalized R_m equation. Section III will discuss the implementation in the RAFT and report and discuss results. Section IV will discuss the adaption of this model to other modes and topologies.

II. Theory

Recently, a generalized expression for the motional parameters of the modified Butterworth van Dyke equivalent circuit was reported [7]. The motional resistance is given by

$$R_m = \frac{\int_V \boldsymbol{S}_n \cdot \boldsymbol{c} \cdot \boldsymbol{S}_n dV}{Q_m \omega_n \int_V \boldsymbol{e}^t \cdot \nabla\phi_{in} \cdot \boldsymbol{S}_n dV \int_V \boldsymbol{e}^t \cdot \nabla\phi_{out} \cdot \boldsymbol{S}_n dV} \quad (1)$$

Where V is the volume of the resonator, S_n is the modal strain from the unity normalized mode shape, e is the piezoelectric matrix, ϕ is the unity normalized electric potential, ω_n is the natural frequency, c is the compliance matrix and Q_m is the mechanical quality factor. *In* and *out* refer to the electric fields for a two-port resonator, with the fields identical for a one port resonator.

The technique here uses the integrals in the denominator of (1) to create an infinite R_m, i.e.

$$\int_V \boldsymbol{e}^t \cdot \nabla\phi \cdot \boldsymbol{S}_n dV = 0 \quad (2)$$

This can occur in two distinct yet mathematically equivalent ways. First, via the direct piezoelectric effect, the charge produced by a strain is proportional to the phase and magnitude of the relevant strain and piezoelectric constants. Therefore, by designing such that equal amounts of positive and negative charges accumulate on the electrode, there is no net current out of the device. Secondly, any mode may be equivalently expressed spatially by mode shapes 180 degrees out of phase with each other. The electric field interacts in certain areas to create a strain that is in a particular phase, and in others to

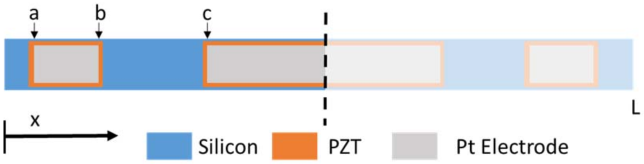

Fig. 1. A top view of the electrode topology utilized to investigate cancellation of chosen modes.

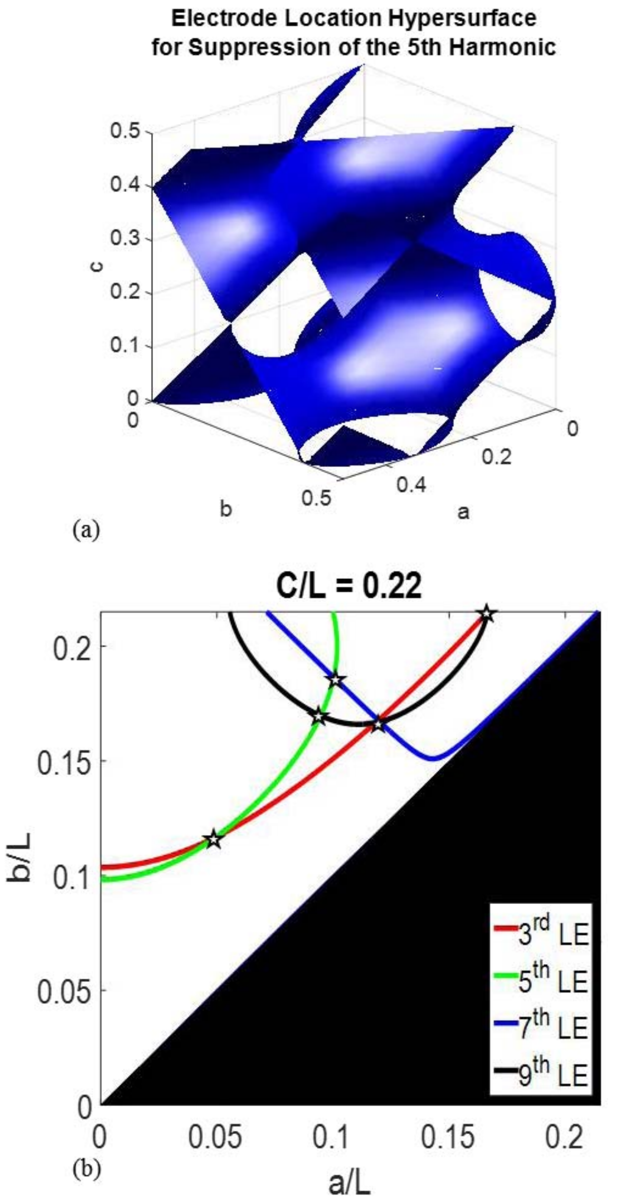

Fig. 2. An example of plots generated from the analytical suppression condition, Equation 4. (a) one hypersurface describing the space of complete suppression for the 5^{th} harmonic. In (b) each curve represents a particular (a,b) coordinate that will results in complete suppression after surfaces like Fig. 2a have been sliced at particular c values. Designs which will suppress multiple modes are marked with stars. A new set of curves is generated when c is changed.

create strains of the opposite phase. If the net contribution to each phase is equal and opposite, the generated waves interfere destructively, and no net strain is generated. In both cases, an electrode shape which creates an electric field which generates no net strain will also accumulate no net charge. Importantly, this also implies that for a two port resonator, the input and output ports may be designed to suppress different modes.

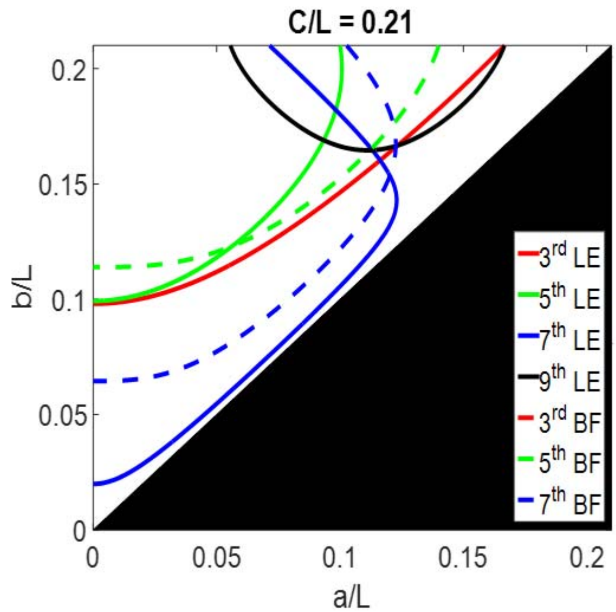

Fig. 3. An example of plots generated from the analytical suppression condition with curves for the suppression of beam flexure included. It may be noted that there are several points which cancel out both beam flexure and length extension harmonics.

A. Length Extension Modes

Length extension (LE) modes may be approximated one-dimensional, i.e. having only one relevant direction of stress/strain. Its modes shapes are harmonics of a cosine function [9]. For length extension modes with parallel plate capacitors creating field in the 3 direction and strain in the 1 direction (II-A) may be simplified to [9]

$$\frac{i\pi}{L}\int_L e_{31}\sin\left(\frac{i\pi x}{L}\right) w_{el}(x)\,dx \tag{3}$$

Where w_{el} is the width of the electrode,[1] i is the harmonic, L is the length of the beam, and e_{31} is the piezoelectric constant.

If a single rectangular electrode is utilized centered about the midplane of Fig. 1, all even harmonics are suppressed. If such an electrode is designed to suppress, say, the 3^{rd} harmonic, analytical formulations predict it will also suppress the 9^{th}, 15^{th}, 21^{st}, etc. harmonics. If designed for the 5^{th} harmonic, it will suppress the 15^{th}, 25^{th}, 35^{th}, etc. harmonics. The issue here is the prime number harmonics above the 2^{nd} harmonic, which would be difficult to suppress if this approach were used. Additionally, the actual fabricated devices do not have ideal mode shapes.

[1] In the work of [1], the width of the electrode is set to $\sin(\pi x/L)$, which is orthogonal to all LE modes except the first harmonic. This has been shown to be quite effective, and a similar idea has been used in [2]. However, the goal of this paper is to demonstrate an algorithm/technique that may be applied across families of modes. Using electrodes with a sine shape is not effective on other modes such as beam flexure. In contrast, this technique can be used to suppress beam flexure, as will be theoretically demonstrated.

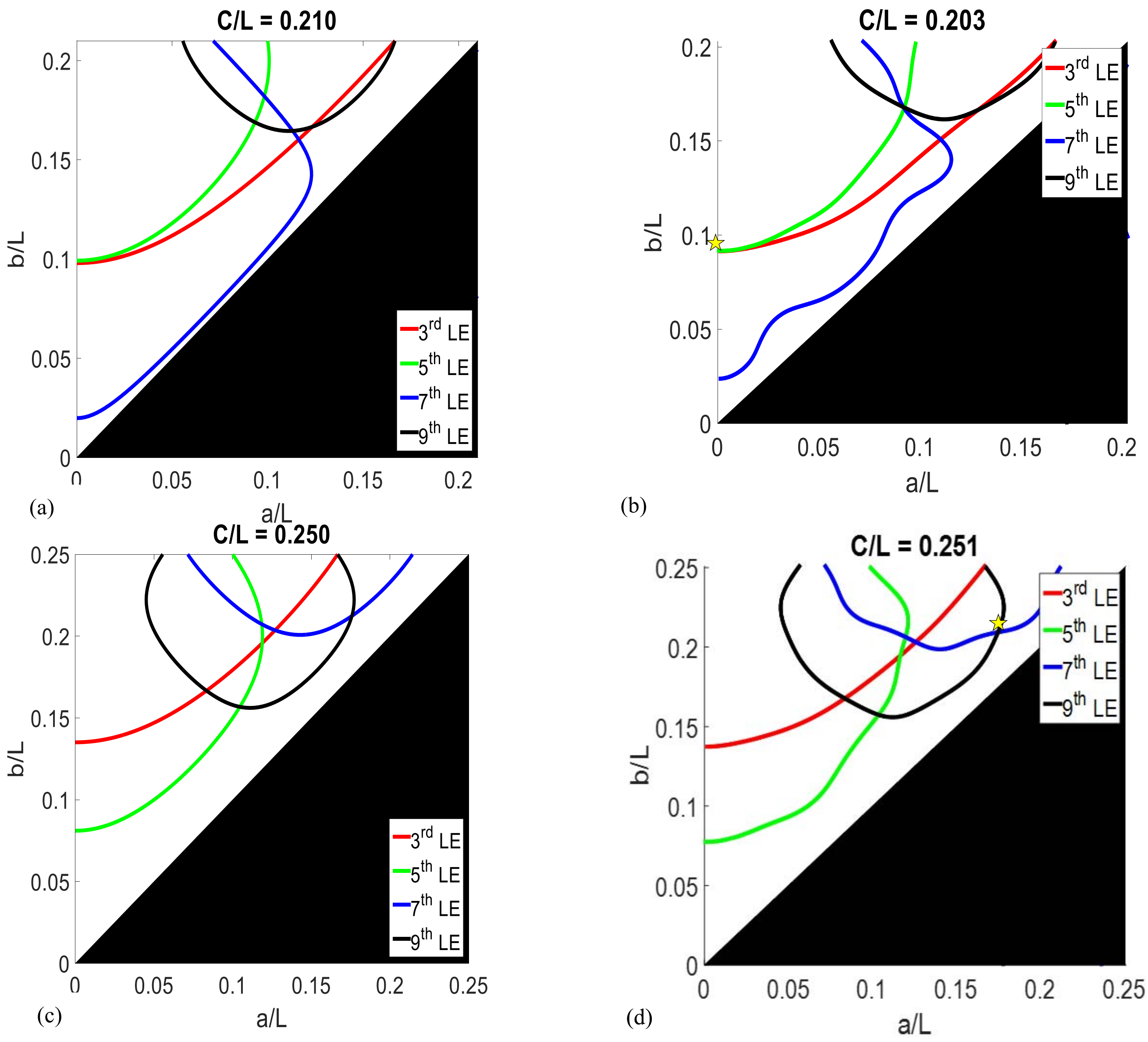

Fig. 4. Spur suppression designs for (a) port 1 using analytical expressions, (b) port 1 using the RAFT, (c) port 2 using analytical expressions, and (d) port 2 using the RAFT. The stars denote the *a* and *b* locations that were designed for in the fabricated device.

By examining the strain shapes of the odd harmonics, a single-electrode design that would suppress the 9$^{\text{th}}$ harmonic was observe to very nearly suppress, for example, the 5$^{\text{th}}$ harmonic. By adding a small block of electrode to straddle a zero strain point of the 9$^{\text{th}}$ harmonic, it was observed that the overlap integral (Eq 2) for the 9$^{\text{th}}$ harmonic would not be affected, but the 5$^{\text{th}}$ harmonic could be reduced. Therefore, to cancel chosen modes, a design similar to that of Fig. 1 was selected and analyzed.

Electroding symmetrically about the midline shown in this figure will suppress even harmonics. The condition for suppression of odd harmonics above the fundamental then becomes

$$\cos\left(\frac{a\pi n}{L}\right)-\cos\left(\frac{b\pi n}{L}\right)+\cos\left(\frac{c\pi n}{L}\right)-\cos\left(\frac{0.5\pi n}{L}\right)=0 \tag{4}$$

This is an implicit function describing a hypersurface, which in this case is a complex 2D surface in 3D space with no analytical solution (Fig. 2a). Note that the fundamental harmonic may not be suppressed due to the strain and charge being all of the same sign.

To explore designs, the location c is set, and a program specifically designed to plot implicit functions is used to graph a and b. This is equivalent to slicing the hypersurface at height c with a plane parallel to the a-b plane. When this is performed, plots like Fig. 2b are produced. Each curve represents all the a and b points which will completely suppress a particular harmonic. To create a design which cancels out multiple harmonics, points where multiple curves intersect should be chosen. Such intersections are labeled with stars in Fig. 2b.

TABLE I
PARAMETERS FOR SPUR SUPPRESSION DESIGN

Variable	*Port 1 Location*	*Port 2 location*
a	0.1	16.6
b	9.2	20.7
c	20.3	25.1

B. Including Other Modes

This technique may be used to suppress modes of other families. For demonstration, beam flexure modes are analyzed theoretically. It is a good candidate as it has a well-known analytical mode shape [9] and is a common spur of length-extension devices. If analysis is carried out to find the condition for complete suppression, hypersurfaces are produced. Designs for both mode families are plotted on the same axes, as seen in Fig. 3. It may be seen that points exist where modes from both families are cancelled simultaneously.

III. SIMULATION AND RESULTS

As proof of concept, only designs suppressing LE harmonics were considered. Discussion of extending this technique to two dimensional modes may be found in section IV.

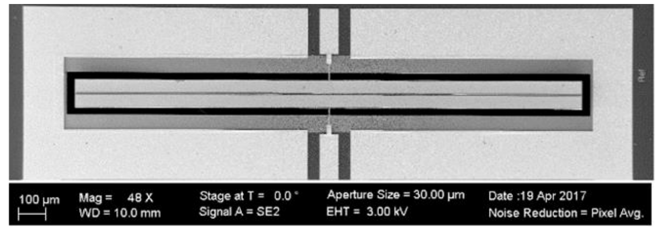

(a)

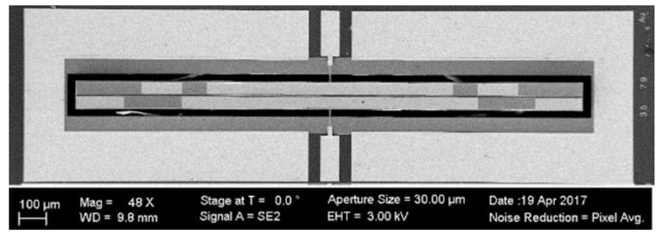

(b)

Fig. 5. (a) The reference design with a common full-length and half-width design. (b) The spurious mode suppression design. One port was designed to suppress length extension harmonics 3 and 5, and the other was designed to suppress harmonics 7 and 9.

A. Simulation

Before fabricating devices, FEA simulation was performed to obtain mode shapes. The simulated and fabricated devices were created in a lead zirconate titanate (PZT)-on-silicon [11] process with of 1 μm buried silicon dioxide, 10 μm of silicon, 300 nm of silicon dioxide, 125 nm of platinum, 0.5 μm of PZT, and 50 nm of platinum. A beam 1872 μm long and 105 μm wide was simulated so that when operating in its 9$^{\text{th}}$ harmonic, the 1D approximation would still hold. When analyzing the resulting mode shapes with a fully covered electrode, the removal of the platinum was assumed to be a negligible perturbation to the mode shape, since the electrode is thin compared to the rest of the stack. Using the RAFT, results generated from FEA are shown in Fig. 4b,d, which is quite similar to Fig. 4a,b (generated from analytical model only). From this analysis, a two-port resonator was designed. Each port was designed to completely suppress two separate modes, for a total of four suppressed modes. A point suppressing 3 modes was not chosen, since only four spurious harmonics were considered. The mode shape of the 11$^{\text{th}}$ harmonic was distorted due to low length to width ratios, creating significant strain in the width.

B. Results

A spurious suppression design and reference design with a common electrode topology were fabricated [3] (Fig. 5). The results from the reference device and suppression devices with one port designed to suppress length extension harmonics 3 and 5 and the other port designed to suppress harmonics 7 and 9 are shown in Fig. 6. The a, b and c locations for the fabricated device are marked with stars and percent values of the 1872 μm long beam are given in Table I.

All scattering (S) parameter measurements were taken on PM5 RF probe station (Cascade Microtech) at atmospheric pressure. 2 port S-parameters were measured using a ZVB-8 Rhode & Schwarz vector network analyzer terminated to 50 Ω. 2 port calibration using short, open, load, and through standards was performed on a GGB CSF-5 ceramic substrate.

Clearly, the fundamental harmonic is minimally impacted by this technique (Fig. 6b). This is due to the highest strain points of the fundamental harmonic remaining electroded, while the lower strain regions had the electrode removed. The Q_m of the reference design was 597. For the spurious mode suppression design, the Q_m was 628. These values were obtained from extraction using Keysight Advanced Design Systems software to fit to the mBVD.

The other targeted modes have been significantly, if not wholly, suppressed (Figs. 6c,d,e,f). The 7$^{\text{th}}$ and 9$^{\text{th}}$ harmonic are nearly completely suppressed, while the 3$^{\text{rd}}$ harmonic is suppressed by 23 dB and the 5$^{\text{th}}$ harmonic is suppressed by 12.5 dB. The incomplete suppression may be from three possible sources. First, the previously discussed assumptions that the removal of platinum is a negligible perturbation to the mode shape will certainly affect suppression. Second, electrode misalignment could reduce the effectiveness of this technique. Finally, the end sections are connected to the mid-section via a very thin platinum trace coated with gold. Voltage drops across this thin section can results in imperfect charge cancellation. The resistivity of the thin trace is calculated to be ∼50 Ω, while the impedance of the capacitor at 20 MHz is ∼10 Ω. This would result in incomplete spurious mode suppression.

To understand why the main resonance remains unaffected, the quality factor and electromechanical coupling, k_{eff}^2, are examined. The electromechanical coupling is given by [12]

$$k_{eff}^2 = \frac{C_m}{C_0 + C_m} \tag{5}$$

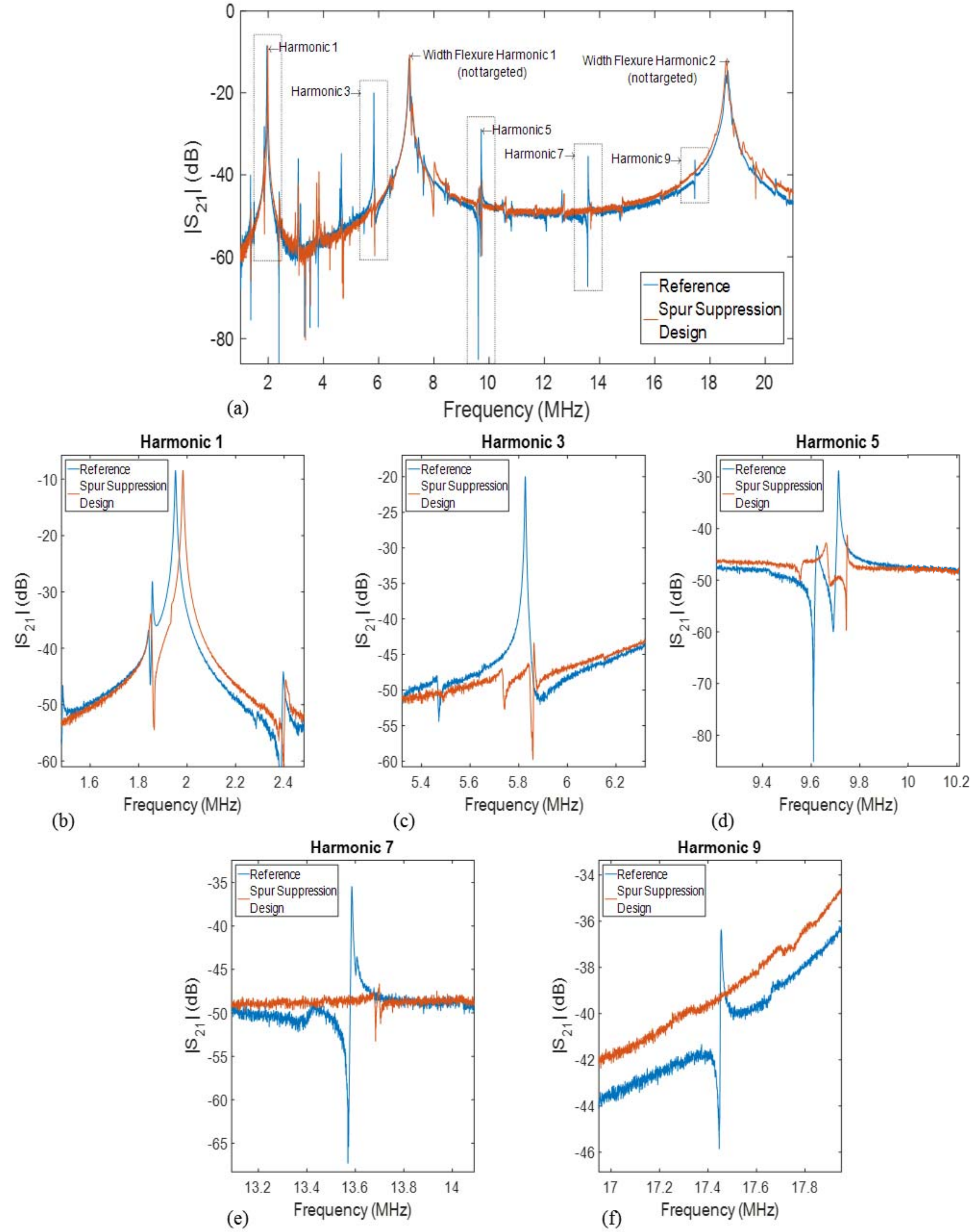

Fig. 6. (a) The wide band measurement of the spurious mode suppression design. The modes near 7 and 19 MHz are harmonics of width flexure, and were not targeted in this analysis. (b) The fundamental mode, which shows minimal impact on its magnitude. Close ups of the (c) third, (d) fifth, (e) seventh, and (f) ninth harmonic of length extension are shown. All modes exhibit significant suppression compared to the reference design.

Here, C_0 is the static capacitance and C_m is the motional capacitance, which is determined from the Q_m relationship with the R_m

$$C_m = \frac{1}{\omega_0 Q_m R_m} = \frac{\int_V \boldsymbol{e}^t \cdot \nabla\phi_{in} \cdot \boldsymbol{S}_n dV \int_V \boldsymbol{e}^t \cdot \nabla\phi_{out} \cdot \boldsymbol{S}_n dV}{\int_V \boldsymbol{S}_n \cdot \boldsymbol{c} \cdot \boldsymbol{S}_n dV} \quad (6)$$

By analyzing the electromechanical coupling using analytical mode shapes, the maximal coupling is obtained for the first harmonic when a single electrode centered about the about the midplane of Fig. 1 spans approximately 75% of the total length. This is because the ends of the beam are low-strain regions. Therefore, the electrodes in the end regions contribute significantly to the static capacitance, but

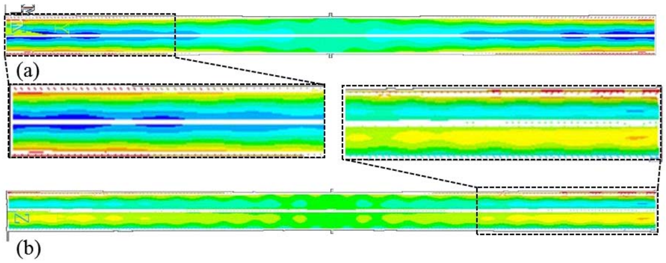

Fig. 7. Top view of the FEA results for the modes labeled as (a) the first harmonic and (b) the second harmonic of width flexure n Fig. 6a. The out of plane displacement profile is plotted along with zoomed in images.

marginally to the motional capacitance. This means that removal of electrodes regions from the end regions of the resonator does not necessarily result in significant reduction in overall coupling. Indeed, an analysis using analytical mode shapes in (3) and (4) predicts that the difference between the reference and spurious suppression design should only be less than 3%. Regarding Q_m, the value is not expected to vary significantly with the removal of PZT and platinum, which are mechanically lossier thank silicon, for two reasons. First, the PZT and platinum make up only about 5% of the total volume. Additionally, only a portion of the total PZT and platinum volumes are removed to design for spurious modes. Secondly, the areas with the highest strain energy density for the fundamental harmonic do not have material removed. Therefore, the mechanical loss effects of PZT and platinum are still expected to contribute significantly to the design for spurious mode suppression. This is reflected in the measured and extracted Q_m stated earlier.

It is also important to note that there are several large spurs which were not much affected by this technique labeled in Fig. 6a as width flexure harmonics. These modes were identified by using the RAFT, and the displacement profiles may be viewed in Fig. 7a,b. The Eigen analysis portion of the RAFT returned the width flexure modes with frequencies very close to the measured frequencies. Additionally, the coupling of these modes calculated from the RAFT was among the highest for all modes, providing further evidence that the modes are correctly identified

With the imposed electrode design, it is not possible to cancel these modes out. In fact, it is not possible at all to cancel out the fundamental width flexure mode with a non-trivial electrode design. This is due to the fact that the strain in the piezoelectric layer/charge produced on the electrode is all of the same sign, and so charge/strain cancellation cannot occur. One possibility to eliminate flexural spurious modes is to fabricate resonators in a stack symmetric about the piezoelectric so no bending moment is generated.

IV. Discussion

The technique demonstrated here has successfully suppressed chosen harmonics of length extension when considering the removal or addition of electrode material produces a negligible perturbation to the mode shape. It has theoretically been shown that the technique can apply to other families of modes as well. However, the results highlight two important questions. The first is how to handle modes which may not be considered one dimensional, or are propagating in the width direction. The other is how to handle the problem of the removal of electrodes exacerbating non-targeted spurious modes.

These questions are very much related as they both require the consideration of the full strain and electric fields. The author would like to suggest one possible solution to this problem. The modification of the electrode will affect *all* modes. This is a very large problem space to consider. For complex electrical fields such as those generated by interdigitated electrodes, (II-A) will not have a simple analytical solution by which to approximate the suppression condition. Additionally, for many modes families it is difficult to derive a closed-form solution for the mode shape. With six dimensions of strain, three dimensions of field, and many modes, an analytical solution is not possible. The simple case of well-behaved, analytic, one-dimensional modes required an implicit solver. Adding an additional electrode "island" would require solving a 5 dimensional implicit equation. These observations point towards a computational solution. The RAFT has already demonstrated its ability to accurately and quickly predict the behavior of many modes across a wide frequency range [7]. In the context of the RAFT, a topological design of the electrodes is performed (the details of the algorithm are beyond the scope of this letter) in similar fashion to prior studies [13], [14]. However, these works only considered if a discrete area would contribute positively or negatively to transduction, but did not account for the degree of contribution as the generalized R_m of the RAFT does or more complex electric fields. The addition and removal of the electrode blocks is treated as a small perturbation to the system. The RAFT will also inform the designer as to the impact of design choices on the coupling of the intended mode. An interesting alternative use of this technique would be to investigate and optimize the coupling of unconventional modes.

Two key advantages of RAFT enable this design procedure. RAFT allows designers to investigate how each individual mode is contributing to the frequency response. Additionally, RAFT allows the re-simulation of the electrical domain independent of the mechanical domain, allowing the treatment of the addition/removal of electrode as a negligible perturbation. These abilities, to the best of the author's knowledge, are not readily available in any other simulation technique. Once an optimal design is arrived at, the mechanical domain of the resonator is re-simulated with the electrode for accurate mode shapes, and the resonator is further refined.

In summary, the technique demonstrated here is a proof-of-concept of the use of the RAFT to design for spurious mode suppression. It has theoretically been shown to suppress modes from other families. However, it will need to be adapted to consider the effect of electrode design on all other modes, modes with several significant degrees of strain, and resonators with more complex electric field. The complexity of the problem points towards an algorithmic approach to a solution, as well as incorporation of other spurious mode suppression techniques.

REFERENCES

[1] A. Prak, M. Elwenspoek, and J. H. J. Fluitman, “Selective mode excitation and detection of micromachined resonators,” *J. Microelectromech. Syst.*, vol. 1, no. 4, pp. 179–186, 1992.

[2] M. Giovannini, S. Yazici, N.-K. Kuo, and G. Piazza, “Spurious mode suppression via apodization for 1 GHz AlN contour-mode resonators,” in *Proc. IEEE Int. Freq. Control Symp. (FCS)*, Baltimore, MD, USA, May 2012, pp. 1–5.

[3] J. S. Pulskamp, S. S. Bedair, R. G. Polcawich, and S. A. Bhave, “Ferroelectric PZT RF MEMS resonators,” in *Proc. IEEE Int. Freq. Control Symp. (FCS)*, San Francisco, CA, USA, May 2011, pp. 1–6.

[4] R. H. Olsson, III, and I. El-Kady, “Microfabricated phononic crystal devices and applications,” *Meas. Sci. Technol.*, vol. 20, no. 1, p. 012002, 2008.

[5] A. Gao and S. Gong, “Harnessing mode conversion for spurious mode suppression in AlN laterally vibrating resonators,” *J. Microelectromech. Syst.*, vol. 25, no. 3, pp. 450–458, 2016.

[6] R. H. Olsson, III, K. E. Wojciechowski, and D. W. Branch, “Origins and mitigation of spurious modes in aluminum nitride microresonators,” in *Proc. IEEE Int. Ultrason. Symp. (IUS)*, San Diego, CA, USA, Oct. 2010, pp. 1272–1276.

[7] A. Link, E. Schmidhammer, H. Heinze, M. Mayer, B. Bader, and R. Weigel, “Appropriate methods to suppress spurious fbar modes in volume production,” in *IEEE MTT-S Int. Microw. Symp. Dig.*, San Francisco, CA, USA, Jun. 2006, pp. 394–397.

[8] J. M. Puder, J. S. Pulskamp, R. Q. Rudy, R. G. Polcawich, and S. A. Bhave, “Orders of magnitude reduction in acoustic resonator simulation times via the wide-band rapid analytical-FEA technique,” in *Proc. Joint Conf. Eur. Freq. Time Forum IEEE Int. Freq. Control Symp. (EFTF/IFCS)*, Besancon, France, Jul. 2017, pp. 807–810.

[9] R. D. Blevins, “Straight beams,” in *Formulas for Natural Freqency and Mode Shape*. Malabar, FL, USA: Krieger, 1983, pp. 108–109.

[10] J. M. Puder, J. S. Pulskamp, R. Q. Rudy, R. G. Polcawich, and S. A. Bhave, “A general analytical formulation for the motional parameters of piezoelectric MEMS resonators,” *IEEE Trans. Ultrason., Ferroelect., Freq. Control*, to be published.

[11] J. S. Pulskamp *et al.*, “Electrode-shaping for the excitation and detection of permitted arbitrary modes in arbitrary geometries in piezoelectric resonators,” *IEEE Trans. Ultrason., Ferroelect., Freq. Control*, vol. 59, no. 5, pp. 1043–1060, May 2012.

[12] B. Jaffe, W. R. Cook, and H. Jaffe, “Piezoelectric ceramics,” in *Measurements Techniques*. Marietta, Georgia: CBLS, 1971, ch. 3, sec. 2, p. 31.

[13] A. Donoso and O. Sigmund, “Topology optimization of piezo modal transducers with null-polarity phases,” *Struc. Multidiscipl. Optim.*, vol. 53, no. 2, pp. 193–203, 2016.

[14] J. L. Sanchez-Rojas *et al.*, “Modal optimization and filtering in piezoelectric microplate resonators,” *J. Micromech. Microeng.*, vol. 20, no. 5, p. 055027, 2010.

Jonathan M. Puder received the B.S. and M.S. degrees in mechanical engineering from Cornell University, Ithaca, NY, USA, in 2012 and 2016, respectively, where he is currently pursuing the Ph.D. degree in mechanical engineering.

He joined the OxideMEMS Group, Cornell University, as an Undergraduate Research Assistant, in 2012, where he is currently a Graduate Research Assistant. He is also a Mechanical Engineer with the PiezoMEMS Group, U.S. Army Research Laboratory, Adelphi, MD, USA, where he has been since 2014. His research interests include piezoelectric MEMS resonance-based devices.

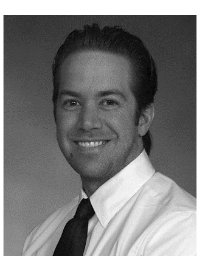

Jeffrey S. Pulskamp received the B.S. degree in mechanical engineering from the University of Maryland, College Park, MD, USA, in 2000. He is currently a MEMS Design and Mechanical Engineer with the Micro and Nano Materials and Devices Branch, U.S. Army Research Laboratory, Adelphi, MD, USA.

He has authored two book chapters on the design and fabrication of piezoelectric MEMS devices, and currently holds ten patents related to piezoelectric MEMS devices and has additional five patents pending. His current research interests include RF MEMS resonators and switches, electromechanical design and modeling of MEMS, and millimeter-scale robotics.

Ryan Q. Rudy received the B.S.E. degree and the M.S.E. degree in mechanical engineering from the University of Michigan, Ann Arbor, MI, USA, in 2009 and 2010, respectively, and the Ph.D. degree in mechanical engineering from the University of Maryland, College Park, MD, USA, in 2014, with a focus on miniaturized ultrasonic motors. He is currently a Mechanical Engineer with the Micro and Nano Materials and Devices Branch, U.S. Army Research Laboratory, Adelphi, MD, USA. His current research interests include piezoelectric MEMS, specifically piezoelectric electromechanical resonators and filters.

Ronald G. Polcawich (SM’07) received the B.S. degree in materials science and engineering from Carnegie Mellon University in 1997, and the M.S. degree in materials and the Ph.D. degree in materials science and engineering from Penn State University in 1999 and 2007, respectively. He is currently a Staff Researcher with the Micro and Nano Materials and Devices Branch, U.S. Army Research Laboratory, Adelphi, MD, USA, where he is also the Team Leader for PiezoMEMS Technology with a focus on developing component technologies to enable cognitive RF communication and radar systems, and MEMS inertial and aiding sensors to provide position, navigation, and timing solutions for SWAP-C constrained platforms. His research activities include materials processing of lead zirconate titanate (PZT) thin films, MEMS fabrication, RF components, MEMS actuator technologies, millimeter-scale robotics, MEMS inertial sensors, and sensors for aiding inertial systems. He has authored over 70 articles and three book chapters on fabrication and design of piezoelectric MEMS devices using PZT thin films. He currently holds 13 patents and has ten patent applications pending review. He received the 2012 Presidential Early Career Award for Scientists and Engineers, and the 2015 IEEE UFFC Ferroelectrics Young Investigator Award.

Dr. Polcawich is a member of the IEEE Ferroelectrics Committee and is the Technical Program Committee IV Applications of Ferroelectrics. He served as an Elected Member of the IEEE Ultrasonics, Ferroelectrics, and Frequency Control Administrative Committee from 2014 to 2016. He has been the Chair of the UFFC Membership Committee since 2016. He is on the Technical Advisory Committee of the PiezoMEMS Workshop. He co-organized the 2013 meeting in Washington, DC, and is a Co-Organizer of the 2018 meeting in Orlando, FL.

Sunil A. Bhave received the B.S. and Ph.D. degrees in electrical engineering and computer science from the University of California at Berkeley, Berkeley, CA, USA, in 1998 and 2004, respectively. He was an Associate Professor with the School of Electrical and Computer Engineering, Cornell University, Ithaca, NY, USA, for ten years. In 2015, he joined the Department of Electrical and Computer Engineering, Purdue University, West Lafayette, IN, USA, as an Associate Professor. His research interests include exploring, understanding, and exploiting interdomain coupling in optomechanical, spin-acoustic, and atom-MEMS systems to design inertial sensors, clocks, and field-programmable microwave chipsets.

Dr. Bhave was a recipient of the National Science Foundation Early CAREER Development Award in 2007, the Defense Advanced Research Projects Agency Young Faculty Award in 2008, and the IEEE Ultrasonics Young Investigator Award in 2014. Along with his students, he received the Roger A. Hakan Best Paper Award at the International Electron Devices Meeting in 2007, and the Student Paper Competition Award at the IEEE International Ultrasonics Symposium in 2009 and the IEEE Photonics Conference in 2012.